

## Accepted Manuscript

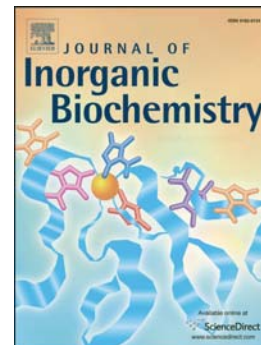
Effects of coordination mode of 2-mercaptothiazoline on reactivity of Au(I) compounds with thiols and sulfur-containing proteins

C. Abbehausen, C.M. Manzano, P.P. Corbi, N.P. Farrell

PII: S0162-0134(16)30134-9  
DOI: doi: [10.1016/j.jinorgbio.2016.05.011](https://doi.org/10.1016/j.jinorgbio.2016.05.011)  
Reference: JIB 10000

To appear in: *Journal of Inorganic Biochemistry*

Received date: 17 February 2016  
Revised date: 13 April 2016  
Accepted date: 13 May 2016



Please cite this article as: C. Abbehausen, C.M. Manzano, P.P. Corbi, N.P. Farrell, Effects of coordination mode of 2-mercaptothiazoline on reactivity of Au(I) compounds with thiols and sulfur-containing proteins, *Journal of Inorganic Biochemistry* (2016), doi: [10.1016/j.jinorgbio.2016.05.011](https://doi.org/10.1016/j.jinorgbio.2016.05.011)

This is a PDF file of an unedited manuscript that has been accepted for publication. As a service to our customers we are providing this early version of the manuscript. The manuscript will undergo copyediting, typesetting, and review of the resulting proof before it is published in its final form. Please note that during the production process errors may be discovered which could affect the content, and all legal disclaimers that apply to the journal pertain.

**Effects of coordination mode of 2-mercaptothiazoline on reactivity of Au(I) compounds with thiols and sulfur-containing proteins**

C. Abbehausen<sup>a\*</sup>, C. M. Manzano<sup>a</sup>, P. P. Corbi<sup>a</sup> and N. P. Farrell<sup>b</sup>

<sup>a</sup>*Institute of Chemistry, University of Campinas - UNICAMP, PO Box 6154, CEP 13083-970, Campinas, SP, Brazil*

<sup>b</sup>*Department of Chemistry, Virginia Commonwealth University, 1001 W. Main St. Richmond, Virginia, 23284-2006, United States*

*\*Corresponding author:*

*Institute of Chemistry – University of Campinas.*

*PO Box 6154, 13083-970, Campinas, SP, Brazil*

*Telephone: + 5519 35213055 / FAX: + 5519 35213023*

*E-mail addresses: camabbehausen@iqm.unicamp.br*

**ABSTRACT**

Gold(I) based drugs are interesting for their potential medical use. The relatively facile ligand substitution in linear gold(I) compounds makes the identification of active species complicated. Ligands such as  $\text{PR}_3$  and  $\text{CN}^-$  are likely to be carrier ligands due to their strong *trans*-directing properties and will dictate the nature of substitution reactions. The 2-mercaptothiazoline (mtz) ligand is an N,S-heterocyclic compound which presents an exocyclic thiol sulfur as well as a heterocyclic nitrogen. The coordination of mzt to transition metals can be modulated by the *trans* ligand and complexes with metal bound through the nitrogen and/or the exocyclic sulfur are known. Therefore, the complexes  $[\text{NCAu}(\text{N-mtz})]$  (N-coordinated) and  $[(\text{Ph}_3\text{P})\text{Au}(\text{S-mtz})]$  (S-coordinated) were investigated to compare the influence of  $\text{CN}^-$  and  $\text{PR}_3$  as well as the coordination mode of the mzt ligand on reactivity with thiols and sulfur-containing proteins. As a further comparison the compound  $[(\text{Ph}_3\text{P})\text{AuCN}]$  was also studied. Human serum albumin, egg white lysozyme and, principally, the C-terminal zinc finger (ZF2) of the nucleocapsid NCp7protein of HIV-1 were studied. Results from zinc finger studies show that the coordination structure can determine the reactivity toward biomolecules. Due to ligand scrambling, the complex  $[\text{NCAu}(\text{N-mtz})]$  forms very reactive species in solution generating  $[\text{NC}_y\text{Au}_x\text{-biomolecule}]$  adducts, where  $x, y \leq 3$ . The observation by mass spectrometry of  $[(\text{CN})\text{Au}]$ -ZF confirms the ability of Au(I) compounds to form  $[(\text{Ligand})\text{Au}]$  adducts on zinc fingers, in contrast to Au(III), where all ligands are lost upon reaction with the zinc finger. On the other hand,  $[(\text{Ph}_3\text{P})\text{Au}(\text{S-mtz})]$  also generates the  $[(\text{Ph}_3\text{P})_2\text{Au}]^+$  species due to ligand scrambling, that showed lower reactivity, probably due to steric hindrance. For this complex  $[(\text{Ph}_3\text{P})\text{Au-biomolecule}]$  and  $[\text{Au-biomolecule}]$  adducts are dominant. The results corroborate the hypothesis of modulation through coordination as the reactivity clearly depends on not only the ligand, but also the coordination mode.

**KEY WORDS:** Gold(I); Sulfur proteins interaction; Zinc finger; 2-Mercaptothiazoline

**INTRODUCTION**

*The structure-activity relationship is an important aspect of drug design. The understanding of the kinetics and thermodynamics of metallodrug speciation in biological systems is essential to unveil their mechanism of action and advance the pharmacology. It is important to consider that the administered complex is not usually the active species, but may be transformed by ligand substitution or redox reactions before it reaches the cellular target. Due to the clinical success of platinum-based anticancer drugs, extensive work on the speciation of platinum complexes have been reported, describing mechanisms of action and also contributing to the design of new Pt(II) or Pt(IV) compounds. [1-5] Studies on speciation of metallodrugs by several techniques as nuclear magnetic resonance (NMR) and mass spectrometry (MS) have*

also contributed to the design of new compounds for the treatment of Alzheimers disease, cancer, bacterial and viral infections and parasitic diseases. [6-10]

Gold(I) based drugs have shown a wide variety of biological properties and medical uses. One of the first compounds to display antibacterial activity was the gold-cyanide ion  $[\text{Au}(\text{CN})_2]^-$ . [11] The intravenously administered gold(I) thiolate polymers, used clinically as anti-arthritic agents for almost 80 years, were augmented in the 1960's by the development of the orally active auranofin. [12] The well-defined structure of auranofin contains the triethylphosphine ( $\text{PEt}_3$ ) ligand and many variations on the basic structure, including modification of the phosphine, have subsequently been examined for multiple biological properties and structure-activity relationships. [13, 14] Anticancer, antiviral, anti-parasitic activities have all been reported for several gold complexes. [13, 15-17] *Due to their wide spectrum of activity, Au(I) and Au(III) compounds have been subjected to several studies to understand their mechanism of action. [14, 18-22] The soft nature of Au(I) and Au(III) ions suggests selenols and thiol-containing proteins as targets, for example thioredoxin, trypanothione, reverse transcriptase, cysteine proteases (cathepsins) and zinc fingers. [14, 17]*

The relatively facile ligand substitution of Au(I) and especially Au(III) compounds means that speciation and identification of active species is complex. [23] Strong *trans*-directing ligands such as  $\text{PR}_3$  and  $\text{CN}^-$  are likely to be carrier ligands as they will dictate substitution reactions in the biological medium. The carrier ligand affects the distribution of gold(I) *in vivo* and  $[\text{Au}(\text{CN})_2]^-$  is a common metabolite of gold(I) drugs. [24] Cyanide can dramatically affect *in vivo* gold distribution compared to  $\text{PR}_3$ . The 2-mercaptothiazoline (mtz) ligand is an N,S-heterocyclic compound that presents an exocyclic sulfur. This molecule exhibits a tautomeric equilibrium in solution with the sulfur in thiol or thione forms (Figure 1B). [25] The coordination of 2-mercaptothiazoline to transition metals can be modulated by the *trans* ligand and complexes with metal bound by the heterocycle nitrogen and/or the exocyclic sulfur are known. [26] The reaction of mzt with  $\text{K}[\text{Au}(\text{CN})_2]$  in acidic conditions results in the nitrogen coordinated complex  $[\text{NCAu}(\text{N-mtz})]$  (**1**, Figure 1A). [27] On the other hand, reaction with  $[(\text{Ph}_3\text{P})\text{AuCl}]$  results in the sulfur coordinated  $[(\text{Ph}_3\text{P})\text{Au}(\text{S-mtz})]$  (**2**, Figure 1A). [28, 29]

To assess the relative reactivity of these coordination modes, we compared their chemistry, along with that of  $[(\text{PPh}_3)\text{Au}(\text{CN})]$  (**3**, Figure 1A) toward N-acetyl-L-cysteine (NAC) and the representative sulfur-containing proteins human serum albumin (HSA), egg-white lysozyme and the C-terminal NCp7 zinc finger of the HIV-1 nucleocapsid protein (NCp7, ZF2) containing the  $\text{Cys}_3\text{His}$  zinc coordination sphere. Previously, the reaction with  $[(\text{PPh}_3)\text{AuL}]^{n+}$  ( $\text{L} = \text{Cl}^-$ ,  $n=0$  and  $\text{L}=\text{substituted pyridine}$ ,  $n=1$ ) with NCp7F2 produced the long-lived species  $[(\text{PPh}_3)\text{Au-peptide}]$  after zinc ejection as well as the predicted gold finger by displacement of the central  $\text{Zn}^{2+}$  with  $\text{Au}^+$ . [22] *The studies were performed by electrospray mass spectrometry (ESI-MS), fluorescence,  $^1\text{H}$ ,  $^{13}\text{C}$  and  $^{31}\text{P}$  NMR, and circular dichroism (CD) spectroscopy.*

## Insert Figure 1

**EXPERIMENTAL***Materials and Equipment*

Compounds **1**, **2** and **3** were synthesized according to literature methods.[27, 28, 30] K[Au(CN)<sub>2</sub>], 2-mercaptothiazoline (mtz), cisplatin, triphenylphosphine (PPh<sub>3</sub>), H[AuCl<sub>4</sub>] and human serum albumin (HSA) were purchased from Sigma Aldrich. C-Terminal HIV-NCp7 apo-peptide was purchased from GenScript Corporation and presents the sequence (KGCWKCGKEGHQMKDCTER), with monoisotopic mass 2224.47 Da. Circular Dichroism (CD) spectra were recorded on a Jasco J-1500 spectrometer (Jasco Analytical Instrumentation, Easton, MD) using the following parameters: measurement range of 240 - 190 nm, data pitch 0.1, CD and FL scales of 200 mdegree/1.0 dOD, data integration time of 4s, bandwidth of 1.00 nm, scanning speed of 20 nm/min. The spectra were accumulated 5 times. Fluorescence experiments were conducted with a Cary Eclipse fluorescence spectrophotometer (Agilent Technologies, Santa Clara, CA) using a cuvette with 10 mm path and volume of 3 mL. The temperature adjustment was made by a Peltier module and magnetic stirring. Zinc fingers were evaluated in a mass spectrometer ThermoElectron Corporation LTQ Orbitrap Velos.

*Reaction with N-acetyl-L-cysteine (NacCys, NAC).*

Solutions containing 35.0  $\mu\text{mol}$  of compounds **1** and **2** were prepared in 0.5 mL deuterated dimethylsulfoxide (DMSO-d<sub>6</sub>). Solutions containing 35.0  $\mu\text{mol}$  of NAC were prepared in 0.5 mL of DMSO-d<sub>6</sub> and added to the complex solutions to obtain a 1:1 molar ratio. The solutions were then transferred to NMR tubes and the <sup>1</sup>H and <sup>31</sup>P (compound **2**) spectra were acquired (time zero). The tubes were kept at 22 °C for 24 h and then new spectra were obtained.

A solution of 35.0  $\mu\text{mol}$  of compound **3** in 0.5 mL CD<sub>3</sub>OD was prepared and the <sup>1</sup>H and <sup>31</sup>P spectra were acquired. The solution was then titrated with sufficient amounts of a 20 mM solution of NAC in CD<sub>3</sub>OD to obtain molar ratios of 1:1, 1:2, 1:3, 1:4 and 1:5. The volume added was 2  $\mu\text{L}$  minimizing the dilution effect. The <sup>1</sup>H and <sup>31</sup>P NMR spectra were acquired immediately upon addition of NAC.

Mass spectra were acquired of 1:1 molar ratio solutions of compounds **1**, **2** and **3** with and without NAC in methanol after incubation in a 37°C water bath. The spectra were obtained in a Waters Quattro Micro API. Samples were evaluated in the positive and negative modes in methanol solution with the addition of 0.10% (v/v) formic acid.

*Fluorescence analysis about the interaction of HSA with compounds 1, 2 and 3.*

The 100  $\mu\text{M}$  solution of HSA (66439 Da) was prepared in 10 mM ammonium acetate. Stock solutions of compounds **1**, **2** and **3** were prepared in methanol to a final concentration of 10 mM. The albumin solutions were titrated with compounds **1**, **2** and **3** and the fluorescence spectrum was acquired in the emission mode with the excitation wavelength of 280 nm and emission recorded in the range of 295 - 500 nm.

#### *Mass spectrometric analyses of the lysozyme interaction with compounds 1, 2 and 3*

A 50  $\mu\text{M}$  solution of lysozyme in 10 mM ammonium acetate was prepared. The mass spectrum of lysozyme was acquired. Stock solutions of compounds **1**, **2** and **3** were prepared in methanol to a final concentration of 10 mmol L<sup>-1</sup>. Sufficient volume of the compounds was added to the lysozyme to reach a final molar ratio 1:1.3. Mass spectra were acquired as soon as the compounds were added (time zero) and after 72 h of incubation at 37 °C.

#### *HIVNCp7-C-terminal zinc finger preparation and interaction with compounds 1, 2 and 3.*

Zinc fingers (ZFs) were prepared for CD and ESI-MS analyzes according to the following procedure: 0.5 mg of the apo-peptide was dissolved in 0.5 mL of degassed water. The concentration based on the isotopic mass was 0.3 mM. A 10 mM stock solution of zinc acetate in degassed water was prepared, and 19.3  $\mu\text{L}$  of this solution was added to the peptide to a final molar ratio of 1:1.3 (peptide/Zn<sup>2+</sup>). The pH was then adjusted to 7.4 with NH<sub>4</sub>OH. The solution was incubated at 37 °C for 2 h and kept in the freezer as a stock for 72 h. Stock solutions of the gold(I) compounds were prepared in methanol for a final concentration of 10 mM. In general, for ESI-MS or CD analyzes the molar ratio 1:1.3 (ZF/Au compound) was used. Titrations for CD analysis were made by adding different volumes of the stock solution of compounds to a stock solution of the ZF to the final molar ratios reported.

#### *Cytotoxicity assays*

Human colon carcinoma (HCT116), human ovarian carcinoma (A2780), human breast cancer (MCF7s), *human astrocytoma grade III (NG97)* and mouse fibroblasts (3T3/Balb) cells were used in this study and maintained according to published procedures [31, 32] The IC<sub>50</sub> values were calculated as described previously.[33] In brief, cells were cultured in RPMI (Gibco, Carlsbad, CA), 5% FBS, 5% BCS and 0.25% penicillin/streptomycin. Cells were routinely passaged at 80 – 90% confluence. For the MTT assay, cells were plated in density of 5000 cells per well in a 96-well plate and incubated overnight at 37 °C in a 5% CO<sub>2</sub> atmosphere. Cells were treated with the complexes in different concentrations for 96 h. Cisplatin, [Au(CN)(mtz)] and [Au(PPh<sub>3</sub>)mtz] were evaluated for comparison. After drug removal, cells were incubated with MTT (3-(4,5-dimethyl-2-thiazolyl)-2,5-diphenyl-2H tetrazolium bromide)

(0.50 mg/mL in RPMI) for 3 h. The excess of MTT was then removed. The dye was dissolved in 100  $\mu$ L of DMSO (Sigma, St Louis, MO), and the absorbance was measured at 540 nm.

## RESULTS AND DISCUSSION

### Reactions with *N*-acetyl-cysteine

Shaw *et al.* extensively studied the displacement, exchange and oxidative reaction of gold drugs with biomolecules.[34-37] Linear gold(I) compounds undergo the ligand scrambling in solution as described in equation 1. In the case of auranofin, the thioglucose is readily displaced by thiolated proteins, mainly HSA.[14] In order to verify and possibly measure the kinetics of the displacement of mtz in reactions with biomolecules of compounds **1** and **2** we first used *N*-acetyl-L-cysteine (NAC) and the reaction was monitored by  $^1\text{H}$  and  $^{31}\text{P}$  NMR.



The  $^1\text{H}$  NMR spectra of compounds **1** and **2** before and immediately after NAC addition show chemical shifts indicative of mtz displacement by the amino acid. (Fig. S1). Specifically, the free mtz ligand presents two triplets centered at 3.87 ppm and 3.50 ppm assigned to hydrogens 4 and 5 respectively.[27] Coordination by the  $[\text{Au}(\text{CN})]$  unit shifts both triplets downfield to 4.20 ppm and 3.67 ppm while similar shifts to 4.30 ppm and 3.39 ppm occur for  $[\text{Au}(\text{PPh}_3)]$  coordination in compound **2** (Figure 2). The  $^{31}\text{P}$  NMR spectrum of compound **2** shifts approximately 2 ppm in the presence of NAC, being consistent with  $[(\text{PPh}_3)\text{Au}(\text{NAC})]$  coordination, Figure 2. The product peak is sharper than that of the precursor, which indicates that compound **2** may be more susceptible to the disproportionation equilibrium, equation 1, than  $[(\text{Ph}_3\text{P})\text{Au}(\text{NAC})]$ . No further changes in the  $^1\text{H}$  and  $^{31}\text{P}$  NMR spectra were observed after 24 h at 25°C indicating that after displacement the products remain stable.

### Insert Figure 2

The chemistry of linear Au(I) compounds in solution is mostly governed by the ligand scrambling shown in equation 1. On the other hand, it was evidenced that  $[(\text{Et}_3\text{P})_2\text{Au}]^+$  formed from the disproportionation of auranofin enters cells and is displaced by sulfur proteins in an oxidative process forming  $\text{Et}_3\text{P}=\text{O}$ , which is a metabolite found in the urine and blood of patients.[24] Considering these facts, and as  $^{31}\text{P}$  and  $^{13}\text{C}$  can be monitored by NMR studies,  $[\text{Ph}_3\text{PAuCN}]$  (compound **3**) is a useful model compound to better understand the relative role of cyanide and phosphine in compounds **1** and **2** respectively.

Compound **3** presents one broad signal in the  $^{31}\text{P}$  NMR spectrum, which indicates the fast disproportionation of  $[\text{Ph}_3\text{PAuCN}]$  to the species  $[(\text{Ph}_3\text{P})_2\text{Au}]^+$  and  $[\text{Au}(\text{CN})_2]^-$ , equation 1,

at room temperature (Figure 3).[38] This is also evidenced in the  $^{13}\text{C}$  NMR spectrum, Figure 4. Upon titration with NAC, the  $^{31}\text{P}$  NMR chemical shift gradually changes, Figure 3. At 1:1 molar ratio displacement of  $\text{CN}^-$  from the species  $[\text{Ph}_3\text{PAuCN}]$  generates the signal at 40.21 ppm, which continuously shifts upfield with increasing concentration of NAC. The chemical shift indicates the formation of the new product  $[(\text{Ph}_3\text{P})\text{Au}(\text{NAC})]$  as well as the starting material, which diminishes with the sequential addition of NAC and the disproportionation product  $[(\text{Ph}_3\text{P})_2\text{Au}]^+$ . Low temperature ( $-75^\circ\text{C}$ ) spectra did not succeed in visualizing the separate signals.[34]

### Insert Figure 3

The  $^{13}\text{C}$  NMR spectrum was acquired for the molar ratio 1:5 ( $[\text{compound}]/[\text{NAC}]$ ) and it was compared with the spectrum of compound **3**, as shown in Figure 4. Compound **3** presents the two  $^{13}\text{C}$  resonances assigned to the  $[\text{Au}(\text{CN})_2]^-$  and  $[\text{Ph}_3\text{PAuCN}]$  in 150.71 ppm and 155.26 ppm respectively, confirming the disproportionation.[38] In the presence of NAC, the signal of compound **3** shows loss of  $\text{CN}^-$  *trans* to the phosphine, being consistent with the  $^{31}\text{P}$  NMR data. A small amount of the  $[\text{Au}(\text{CN})_2]^-$  is still present, suggesting that this is a less reactive species than compound **3** whose signals disappear first.

### Insert Figure 4

#### *Reactions with proteins*

Human serum albumin (HSA) is the most abundant protein in the blood plasma and acts as a carrier of molecules in the organism.[39] It plays important roles in the distribution, free concentration, excretion, metabolism and interaction with the target tissues of a great diversity of drugs, and it has been reported to be essential in the transport and distribution of gold(I) drugs.[14] Studies have demonstrated that the binding site of gold(I) drugs in HSA is the cysteine-34.[40] Other weaker binding sites seem to be dependent on the nature of the gold complex. Auranofin binds exclusively to cys-34 by replacement of the thiosugar moiety. [40] Structurally, HSA is a nonglycosylated protein consisting of a single peptide chain of 585 amino acids, largely helical (67%), with the remaining polypeptide occurring in turns and extended or flexible regions between sub-domains with no  $\beta$ -sheets and having around 66 kDa mass, which organizes itself to form a heart-shaped protein.[39] HSA consists of three homologous domains, namely, I (residues 1e195), II (196e383), and III (384e585), each domain being divided into sub-domains A and B, and the overall structure is stabilized by 17 disulfide bridges. HSA contains a single intrinsic tryptophan residue at position 214 in domain IIA, where a large hydrophobic cavity is present, and its fluorescence is sensitive to the ligands bonded nearby

and structural changes caused by covalent interaction on the protein. [41] In this work, we studied the interaction of compounds **1**, **2** and **3** with human serum albumin by fluorescence.

The fluorescence emission spectra of HSA with different stoichiometric ratios of compounds **1**, **2** and **3** were acquired. A significant quenching is observed for all compounds without changes in the maximum emission wavelength. The quenching was treated by the Stern-Volmer equation as shown in equation 2:

$$F_0/F = 1 + K_{sv} [\text{compound}] \quad [2]$$

where  $F_0$  and  $F$  are the fluorescence intensities in the absence and presence of the quencher,  $K_{sv}$  is the Stern-Volmer quenching constant and  $[\text{compound}]$  is the concentration of the quencher.[42] The Stern-Volmer plots for the three compounds are shown in Figure 5A. Two mechanisms are possible for the fluorescence quenching, the dynamic collision and the formation of complex also known as static. Both of them generate a straight line when  $F_0/F$  is plotted against the quencher concentration. However, when both mechanisms are present the plot presents an upward curvature. As can be observed in Figure 5A, all the compounds present an upward curvature, which is more pronounced in compound **2**, indicating that the dynamic and static mechanisms of quenching are present.

The formation of complex (static mechanism) can be evaluated by the modified Stern-Volmer equation:

$$F_0/\Delta F = F_0/(F_0 - F) = 1/f_a K_a 1/[Q] + 1/f_a \quad [3]$$

The parameter  $K_a$  is analogous of associative binding constant.[42] The modified Stern-Volmer plots are presented in Figure 5B and the deduced  $K_a$  values as the linear correlation coefficient are presented in Table 1. The estimated values are of the order  $10^4$ , which is a moderately strong affinity between the compounds and HSA.

When small molecules bind independently to a set of equivalent sites on a macromolecule, the equilibrium between free and bound molecules is given by the equation 4:

where  $K_b$  and  $n$  are the apparent binding constant and the number of binding sites respectively.[42]

$$\log ((F_0-F)/F) = \log K_b + n \log [\text{compound}] \quad [4]$$

As can be seen in Figure 5C and summarized in Table 1 the number of binding sites is one for compounds **1** and **3** and two for the compound **2**. Compounds **1** and **3** have cyanide as a ligand and the higher binding constant agrees with the reported results that aurocyanide binds strongly enough to albumin to reduce the dicyanoaurate anion in the blood stream but is labile enough to increase the uptake in the red blood cells. These results confirm that the presence of cyanide in the gold(I) complexes increases the binding to sulfhydryls and the slightly

higher  $K_b$  of compound **1** can be the result of the more labile ligand (mtz) in comparison to the phosphine of compound **3**.

### Insert Figure 5

### Insert Table 1

To examine in detail the gold compound-protein interactions, egg white lysozyme was used as protein substrate. It was chosen due to its lower molecular weight (14.3 KDa) when compared to HSA (~66.5 KDa) thus allowing a more sensitive measurement. Further, lysozyme has found recent use as an excellent model system for studying the mechanism of action of cytotoxic Au(III) compounds including X-ray structural characterization of the reduced Au(I) adducts and clear confirmation that the nature of the coordinated ligands plays a key role in the protein-metallodrug recognition process [43, 44]

The studies of compounds **1-3** with lysozyme show a very distinct dependence on the structure with a clear difference in reactivity between the three species with significant reaction only observed for compound **1**. The mass spectrum of lysozyme shows three sets of peaks representing 7+, 8+ and 9+ charges, corresponding to mass in the range 14304.6 Da – 14448 Da. The interactions of the protein with compounds **1-3** were evaluated by acquisition of the spectra right after the addition of the compound. It is possible to observe an immediate reaction of compound **1** with lysozyme, forming adducts of the protein with  $[\text{Au}(\text{CN})_2]^-$  (Figure 6B). The product peaks from the interaction of compound **1** and lysozyme after 72 h are cleaner and the adducts were identified as  $[\text{Lyso} + \text{Au}(\text{CN})_2]^{8+}$  centered at  $m/z$  1822.9 and  $[\text{Lyso} + 2(\text{Au}(\text{CN})_2)]^{8+}$  centered at 1859.7 (Figure 6C). The data are consistent with the binding parameter observed by interaction with albumin. How the  $[\text{Au}(\text{CN})_2]^-$  ion is formed in solution is of interest and the result also suggests an association rather than covalent interaction, which would require displacement of one  $\text{CN}^-$  ligand. In contrast to **1**, compounds **2** and **3** do not show immediate reaction and adduct formation (Figure S2). Even with incubation up to 72h compound **2** does not react, while for compound **3** only adducts with very low intensity centered at  $m/z$  1828.3 and possibly assigned to cyano gold species are seen (Figure S3). It was not the objective to examine the structural details but rather to examine kinetic differences.

The interactions of the Au(I) drugs aurothiomalate and auranofin with lysozyme have also been studied where they behave quite differently.[45] Only non-covalent interactions were found between the polymeric aurothiomalate and non-covalent and covalent adducts were found for auranofin. Also, the interaction between lysozyme and gold(I/III) compounds depends on the nature of the gold starting material, and can be modulated by metallation of the ligands, mainly in gold(I) compounds.[43-45] The results found for compounds **1**, **2** and **3** corroborate this observation.

## Insert Figure 6

*Interaction with HIV-1-NCp7 model peptide.*

Continuing the systematic studies of the interaction of HIV-1-NCp7 with gold(I) compounds, [22], the interaction of compounds **1-3** with the C-terminal-NCp7 zinc finger (ZF) were investigated to understand the role of cyanide *versus* phosphines in the zinc ejection and ligand loss of the complexes. Conformational changes were evaluated by CD and the binding at the molecular level was evaluated by mass spectrometry. Figure 7 shows the CD spectra of C-term-NCp7 and its reaction with increasing concentrations of each compound.

The apoNCp7 presents the typical random coil spectrum with a negative ellipticity centered at 195–200 nm.[10,22,46,47] Zinc(II) coordination to the peptide in a tetrahedral environment decreases the intensity with a slight red shift at 200–210 nm, a positive signal at 190 nm, and a broad and low intensity positive band centered at 225 nm indicating the typical knuckle conformation of NCp7, Figure 7. [10,22,46,47] With compounds **1** and **2** at different stoichiometric ratios a progressive reduction on the positive bands at 190 nm and 225 nm and a blue shift of the band centered in 210 nm to 200 nm are observed (Figure 7A,B). Especially, the loss of the positive signal is indicative of conformational changes with Au(I) and Au(III) compounds.[10] This result suggests the loss of the zinc knuckle structure with the metal coordinated in a tetrahedral geometry to a less organized structure, which can represent one or more gold ion coordinated in a linear geometry to the cysteines and the histidine present in the peptide sequence. On the other hand, compound **3** did not show a pronounced decrease in the positive bands and no shift was observed in the intense negative band, which suggests that no zinc ejection could be observed by this technique.

*The deconvoluted ESI-MS from the immediate reaction of compounds 1-3 with the C-terminal HIV-NCp7 zinc finger is shown in Figure 8, where F represents finger formation, gold finger (AuF) and zinc finger (ZF). The non-deconvoluted spectra showing ions of charge 5<sup>+</sup>, 4<sup>+</sup>, 3<sup>+</sup> and 2<sup>+</sup> are presented in Figure S4. For compound 1 all peaks resulting from Au displacement of Zn correspond to a mixture of Au<sub>x</sub>F (x = 1, 2 or 3) peaks with lower intensity neighbors representing (NC)<sub>y</sub>Au<sub>3</sub>F (y = 1,2,3) as shown for the x = 3 case, Figure 8A. The unique [Zn-AuF]<sup>+</sup> species, which might be an intermediate, and low-intensity apo-peptide can be observed but no intact unreacted ZF was found.*

*For compound 2 the single charged high ionizable species [(Ph<sub>3</sub>P)<sub>2</sub>Au]<sup>+</sup> at m/z 721 is observed upon reaction with ZF (Figure 8B). In this case, the equilibrium shown in equation 1, is shifted to the formation of [(Ph<sub>3</sub>P)<sub>2</sub>Au]<sup>+</sup> not only by the addition of the peptide but also by the ionization process in mass spectrometry. This species is the least reactive probably due to*

steric hindrance. Product peaks are consistent with the reaction of  $(\text{Ph}_3\text{P})\text{Au}(\text{mtz})$  forming the species  $[\text{Au}_n\text{F}]^+$  and  $[(\text{Ph}_3\text{P})\text{AuF}]^+$ . Any  $[\text{Au}(\text{mtz})_2]^+$  formed by disproportionation is likely to contribute to formation of  $[\text{Au}_n\text{F}]$  although the species itself was not observed in the spectrum. The  $[\text{Zn-AuF}]^+$  is also observed for compound **2**, as well as the unreacted ZF, and a very low intense peak of the apo-peptide. These results are consistent with previous studies on  $[(\text{PPh}_3)\text{AuL}]$  where  $\text{L} = \text{Cl}^-$  and N-heterocycles.[22]

### Insert Figure 8

The main characteristic of the reaction of ZF with compound **3** is the presence of high abundance peaks of the disproportionation product, as well as the free unreacted zinc finger. The main products of the reaction are  $[\text{Au}_n\text{F}]^+$  and  $[(\text{Ph}_3\text{P})\text{AuF}]^+$ . Considerable amounts of apo-peptide are also observed, and very low abundance is found for  $\text{NCAuF}$ . The intermediate species  $[\text{Ph}_3\text{PAuZnF}]^+$  is also found in low abundance. Overall, the results suggest a less reactive species in solution resulting from disproportionation and consequently less adduct formation from the immediate reaction. The two ligands are strong donors and strong  $\pi$  acceptors, suggesting stronger interactions.

### Cytotoxicity

The cytotoxicities of the compounds **1** and **2** were evaluated over four different tumorigenic cell lines and one non-tumorigenic line (3T3/Balb) and compared to cisplatin, Table 2. The strains evaluated were the human ovarian carcinoma (A2780), human colon carcinoma (HCT116), human breast adenocarcinoma (MCF7) and the human astrocytoma grade III. The  $\text{IC}_{50}$  values for HeLa cells have been previously reported for compound **1** and are presented for comparison.[27]

### Insert Table 2

Compound **1** inhibited the growth of all tumorigenic cell lines. The  $\text{IC}_{50}$  values vary from  $0.009 \mu\text{M}$  –  $11.0 \mu\text{M}$  depending on the strain. The ovarian carcinoma A2780 was the most sensitive ( $0.009 \mu\text{M}$ ) and the astrocytoma cells were the most resistant ( $11 \mu\text{M}$ ). However, in comparison to the non-tumorigenic 3T3 cells, the astrocytoma strain presented a reasonable  $\text{IC}_{50}$  and the compound **1** showed a significant selectivity. Astrocytomas are extremely aggressive malignancies of the central nervous system (CNS), accounting for 46% of all primary malignant

brain tumors and are very resistant to all chemotherapeutic treatments. Considering this scenario, they can be considered sensitive to compound 1. All cell lines were more sensitive to compound 1 than to cisplatin. Among the cells evaluated, A2780 (ovarian carcinoma) is the most sensitive to all tested compounds. However, it is approximately 25 times more sensitive to compound 1 than to cisplatin with an  $IC_{50}$  in the nanomolar range. Comparing compound 1 and 2, no significant differences were observed in the  $IC_{50}$  values, suggesting that the ligand (phosphine or cyanide) makes no significant difference. Similar values were reported for a series of phosphine compounds with N-heterocyclic ligands evaluated over HCT116, A2780 and MCF7.[22]

ACCEPTED MANUSCRIPT

## SUMMARY AND CONCLUSIONS

Overall, the results show that the structure can determine reactivity on sulfur-containing albumin, lysozyme and ZF proteins, even in the presence of complicating disproportionation reactions. The results show that the compound **1**, after the loss of mtz, forms the  $[\text{AuCN}]$  unit, which is a very reactive species in solution, as observed in the interaction with albumin, lysozyme, and ZF. In the specific case of the zinc finger, it is the only compound that shows multiple gold(I) ions coordinated to the sulfur-rich template as well as several possible  $\text{Au}_x(\text{CN})_y$  species, which may suggest several steps of ligand scrambling. In the case of compound **2**, ligand scrambling produces the species  $[(\text{Ph}_3\text{P})\text{Au}]^+$  with low reactivity probably due to hysteric hindrance. The reactive species are  $[(\text{Ph}_3\text{P})\text{Aumtz}]$  and  $[\text{Au}(\text{mtz})_2]^+$  as can be seen by the species generated  $[\text{AuF}]^+$  and  $[(\text{Ph}_3\text{P})\text{AuF}]^+$ . The affinity is even lower for compound **3** that showed higher stability in the presence of lysozyme and ZF, which is indicated by the high abundant peaks of the free compound and ZF. Interestingly, the cyanide is almost completely lost in the interaction with ZF and only AuF and  $\text{Ph}_3\text{PAuF}$  is found. In addition, the interaction of compound **3** with N-acetyl-L-cysteine shows loss of cyanide as well as in the zinc finger.[27]

This paper corroborates the hypothesis of the modulation through coordination previously discussed by Messori *et al.* in the interaction of lysozyme, cytochrome c, and RNase. [28, 30, 35] The mtz, when coordinated to gold(I) by the nitrogen atom, is more labile and generate reactive species, which metalates pronely sulfur proteins, as HSA and lysozyme. However, the phosphine derivative, coordinated by sulfur, does not interact with lysozyme and has less affinity to ZF. The compound **1** is the second example of an Au-L compound bonded to sulfur proteins, which corroborates to the hypothesis that Au(III) loses all ligands when reduced in biological media prior to the protein interaction and the reactivity of Au(I) depends on the nature of the ligands coordinated.[30] Moreover, compound **3** showed that the combination of two good donors and good  $\pi$  acceptor ligands decreases the reactivity even more, as it is possible to observed by the reaction with lysozyme and ZF.

*In summary, the main finding here is that the affinity for biomolecules is dependent on the ligand and mode of coordination. The data also reinforce the fact that gold(I) compounds act as prodrugs likely to suffer a series of ligand scrambling reactions before reaching the target. The first interaction is probably with HSA resulting in a replacement of the most labile ligand by cysteines in this protein. Zinc fingers are shown to be possible targets and they present even higher affinities than for lysozyme. Compounds containing cyanide can generate the reactive  $\text{AuCN}$  or  $[\text{Au}(\text{CN})_2]$  in solution, which can interact by electrostatic or covalent bonds. On the other hand, phosphines decrease the reactivity, as evidenced by the reaction with lysozyme. Overall, the data represent important information for the design of more specific gold(I) compounds.*

**ACKNOWLEDGEMENTS**

This work was supported by the Brazilian Coordination Agency for the Improvement of High-Level Personnel (CAPES), AUXPE/PVES 0580/2013, São Paulo Research Foundation (FAPESP), processes 2012/08230-2 and 2013/20334-0 and NSF CHE-1413189. The authors thank K. Nelson and K. Knitter for the mass spectrometry analysis, E.J. Peterson, D. Machado and Professor Marcelo Lancellotti for cytotoxicity evaluation and R.E.F. de Paiva for text revision and graphical abstract.

ACCEPTED MANUSCRIPT

## BIBLIOGRAPHY

- [1] E. Wexselblatt, D. Gibson, J. Inorg. Biochem. 117 (2012) 220-229.
- [2] S. Berners-Price, L. Ronconi, P.J. Sadler. Prog. NMR Spec. 49 (2006) 65-98.
- [3] M.D. Hall, T.W. Hambley. Coord. Chem. Rev. 232 (2002) 49-67.
- [4] E. Schreiber-Brynzak, V. Pichler, P. Heffeter, B. Hanson, S. Theiner, I. Lichtscheidl-Schultz, C. Kornauth, L. Bamonti, V. Dhery, D. Groza, D. Berry, W. Berger, M. Galanski, M.A. Jakupec, B.K. Keppler, Metallomics (2016) . [Epub ahead of print]. PMID: 26860208
- [5] A.V. Karotki, M. Vašák, JBIC Journal of Biological Inorganic Chemistry 14 (2009) 1129-1138.
- [6] C.A. Wootton, C. Sanchez-Cano, H.-K. Liu, M.P. Barrow, P.J. Sadler, P.B. O'Connor, Dalton Transactions 44 (2015) 3624-3632.
- [7] T. Zou, P.J. Sadler, Drug Discovery Today: Technologies 16 (2015) 7-15.
- [8] G. Meloni, A. Cramer, G. Fritz, P. Davies, D.R. Brown, P.M.H. Kroneck, M. Vašák, ChemBioChem 13 (2012) 1261-1265.
- [9] S.D. Tsotsoros, A.B. Bate, M.G. Dows, S.R. Spell, C.A. Bayse, N.P. Farrell, J. Inorg. Biochem. 132 (2014) 2-5.
- [10] S.R. Spell, N.P. Farrell, Inorg. Chem. 54 (2015) 79-86.
- [11] T.G. Benedek, J. Hist. Med. Allied Sci. 59 (2004) 50-89.
- [12] A.J. Lehman, J.M. Esdaile, A.V. Klinkhoff, E. Grant, A. Fitzgerald, J. Canvin, M.S.G. The, Arthritis Rheum. 52 (2005) 1360-1370.
- [13] C.K. Mirabelli, D.T. Hill, L.F. Faucette, F.L. McCabe, G.R. Girard, D.B. Bryan, B.M. Sutton, J.O.L. Barus, S.T. Crooke, R.K. Johnson, J. Med. Chem. 30 (1987) 2181-2190.
- [14] C.F. Shaw, Chem. Rev. 99 (1999) 2589-2600.
- [15] T. Okada, B.K. Patterson, S.-Q. Ye, M.E. Gurney, Virology 192 (1993) 631-642.
- [16] M. Navarro, Coord. Chem. Rev. 253 (2009) 1619-1626.
- [17] S.J. Berners-Price, A. Filipovska, Metallomics 3 (2011) 863-873.
- [18] S.M. Meier, C. Gerner, B.K. Keppler, M.A. Cinellu, A. Casini, Inorg. Chem. (2016)
- [19] U.A. Laskay, C. Garino, Y.O. Tsybin, L. Salassa, A. Casini, Chem. Commun. 51 (2015) 1612-1615.
- [20] F. Mendes, M. Groessl, A.A. Nazarov, Y.O. Tsybin, G. Sava, I. Santos, P.J. Dyson, A. Casini, J. Med. Chem. 54 (2011) 2196-2206.
- [21] S.R. Spell, N.P. Farrell, Inorg. Chem. 53 (2014) 30-32.
- [22] C. Abbehausen, E.J. Peterson, R.E.F. de Paiva, P.P. Corbi, A.L.B. Formiga, Q. Yun, N.P. Farrell, Inorg. Chem. 52 (2013) 11280-11287.
- [23] S.M. Cottrill, H.L. Sharma, D.B. Dyson, R.V. Parish, C.A. McAuliffe, J. Chem. Soc., Perk. Trans. 2 (1989) 53-58.

- [24] R.C. Elder, Z. Zhao, Y. Zhang, J.G. Dorsey, E.V. Hess, K. Tepperman, J. Rheumatol. 20 (1993) 268-272.
- [25] C. Abbehausen, R.E.F. de Paiva, A.L.B. Formiga, P.P. Corbi, Chem. Phys. 408 (2012) 62-68.
- [26] R. Uson, A. Laguna, M. Laguna, J. Jimenez, M.P. Gomez, A. Sainz, P.G. Jones, J. Chem. Soc., Dalton Trans. (1990) 3457-3463.
- [27] C. Abbehausen, J.F. Castro, M.B.M. Spera, T.A. Heinrich, C.M. Costa-Neto, W.R. Lustri, A.L.B. Formiga, P.P. Corbi, Polyhedron 30 (2011) 2354-2359.
- [28] U.E.I. Horvath, S. Cronje, S.D. Nogai, H.G. Raubenheimer, Acta Crystallogr. Sect. E: Struct. Rep. Online 62 (2006) m1641-m1643.
- [29] U.E.I. Horvath, H.G. Raubenheimer, Acta Crystallogr. Sect. E: Struct. Rep. Online 62 (2006) m1644-m1645.
- [30] A.L. Hormann, C.F. Shaw, D.W. Bennett, W.M. Reiff, Inorg. Chem. 25 (1986) 3953-3957.
- [31] L.R. Kelland, C.F.J. Barnard, K.J. Mellish, M. Jones, P.M. Goddard, M. Valenti, A. Bryant, B.A. Murrer, K.R. Harrap, Cancer Res. 54 (1994) 5618-5622.
- [32] L.R. Kelland, M. Jones, G. Abel, M. Valenti, J. Gwynne, K.R. Harrap, Cancer Chemother. Pharmacol. 30 (1992) 43-50.
- [33] T. Mosmann, J. Immunol. Methods 65 (1983) 55-63.
- [34] A.L. Hormann-Arendt, C.F. Shaw III, Inorg. Chem. 29 (1990) 4683-4687.
- [35] S. Ahmad, Coord. Chem. Rev. 248 (2004) 231-243.
- [36] S. Ahmad, A.A. Isab, H.P. Perzanowski, Can. J. Chem. 80 (2002) 1279-1284.
- [37] D.T. Hill, A.A. Isab, D.E. Griswold, M.J. DiMartino, E.D. Matz, A.L. Figueroa, J.E. Wawro, C. DeBrosse, W.M. Reiff, R.C. Elder, B. Jones, J.W. Webb, F.C. Shaw III, Inorg. Chem. 49 (2010) 7663-7675.
- [38] A.A. Isab, M.S. Hussain, M.N. Akhtar, M.I.M. Wazeer, A.R. Al-Arfaj, Polyhedron 18 (1999) 1401-1409.
- [39] X.M. He, D.C. Carter, Nature 358 (1992) 209-215.
- [40] J. Christodoulou, P.J. Sadler, A. Tucker, FEBS Lett. 376 (1995) 1-5.
- [41] Y.V. Il'ichev, J.L. Perry, J.D. Simon, J. Phys. Chem. B 106 (2002) 452-459.
- [42] J.R. Lacowicz, in: S.S. Media (Ed.) Book Principles of Fluorescence Spectroscopy, Springer US, New York, 2006, 3-984
- [43] C. Gabbiani, L. Massai, F. Scaletti, E. Michelucci, L. Maiore, M.A. Cinellu, L. Messori, J. Biol. Inorg. Chem. 17 (2012) 1293-1302.
- [44] L. Messori, F. Scaletti, L. Massai, M.A. Cinellu, C. Gabbiani, A. Vergara, A. Merlino, Chem. Commun. (Camb.) 49 (2013) 10100-10102.
- [45] F. Darabi, T. Marzo, L. Massai, F. Scaletti, E. Michelucci, L. Messori, J. Inorg. Biochem. 149 (2015) 102-107.
- [46] Q.A. de Paula, J.B. Mangrum, N.P. Farrell, J. Inorg. Biochem. 103 (2009) 1347-1354.
- [47] S.M. Quintal, Q.A. dePaula, N.P. Farrell, Metallomics 3 (2011) 121-139.

[48] T.A. Heinrich, G. Von Poelhsitz, R.I. Reis, E.E. Castellano, A. Neves, M. Lanznaster, S.P. Machado, A.A. Batista, C.M. Costa-Neto, Eur. J. Med. Chem. 46 (2011) 3616-3622.

ACCEPTED MANUSCRIPT

## FIGURES AND TABLES CAPTIONS

Figure 1. (A) Structures of the studied compounds **1**, **2**, **3** and auranofin. (B) Tautomeric equilibrium of the ligand 2-mercaptthiazoline (mtz) in solution.

Figure 2. (A)  $^{31}\text{P}$  NMR spectra of compound **2** and compound **2** + NAC. (B)  $^1\text{H}$  NMR (region 3.2 ppm to 4.6 ppm) of compound **2** and compound **2** + NAC. The mtz is shown for reference.

Figure 3.  $^{31}\text{P}$  NMR spectra of compound **3** with different amounts of NAC. Spectra were recorded immediately after addition of NAC at the molar ratio indicated. All spectra were recorded in  $\text{CD}_3\text{OD}$  and referenced to  $\text{H}_3\text{PO}_4$ .

Figure 4.  $^{13}\text{C}$  NMR spectra (region 147 ppm – 162 ppm) of compound **3** and compound **3** + NAC in 1:5 molar ratio. Spectra acquired in  $\text{CD}_3\text{OD}$ , number of scans 10240.

Figure 5. (A) Stern-Volmer plot for quenching HSA with compounds **1-3** in buffer solution (B) The modified Stern-Volmer plots of HSA of compounds **1-3**. (C) Double-log plots of compounds **1-3** quenching effect on HSA fluorescence

Figure 6. ESI-MS spectra of lysozyme + compound **1**. (A) lysozyme, (B) lysozyme + compound **1** – time zero (C) lysozyme + compound **1** – 72h. Lysozyme molecular weight (amino acid sequence) 14304 Da.  $m/z$  1789.1 = mass 14304.6 Da.

Figure 7. Circular dichroism spectra of C-terminal NCp7 ZF titrated with different amounts of compounds **1-3**. Molar ratios indicated on graphs. (A) Spectra of apo-peptide and NCp7, showing the formation of the ZF. (B) NCp7 titrated with compound **1**. (C) NCp7 titrated with compound **2**. (D) NCp7 titrated with compound **3**.

Figure 8. Deconvoluted ESI-MS spectra of the C-terminal NCp7 ZF + compounds **1 - 3**. Spectrum A - compound **1**; spectrum B - compound **2**; spectrum C - compound **3**. Insert graphs are amplifications of the regions indicated. ZF indicates the zinc finger, and AuF indicates the gold finger. Apo-NCp7 or apo indicates the free peptide with no metal.

Table 1. Modified Stern-Volmer association constant  $K_a$  and respective linear correlation coefficient. Binding parameters,  $n$  and  $K_b$ , for the system HSA with compounds **1-3** and respective linear correlation coefficient. (a) Linear correlation coefficient for modified Stern-Volmer plots. (b) Linear correlation coefficient for double log plots of the quenching effects.

Table 2.  $\text{IC}_{50}$  values for  $[\text{NCAu}(\text{N-mtz})]$ , **1**, and  $[(\text{PPh}_3)\text{Au}(\text{S-mtz})]$ , **2** in different tumorigenic cell lines and the non-tumorigenic line 3T3 obtained by MTT assay. Cisplatin was also evaluated for comparison.

Figure 1

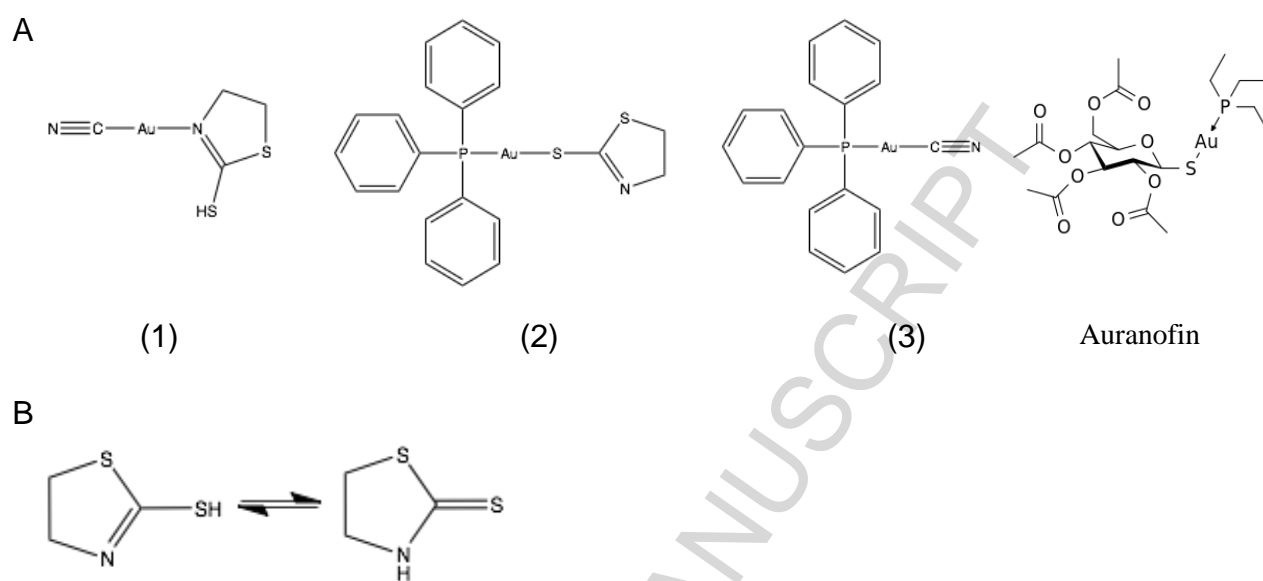


Figure 2

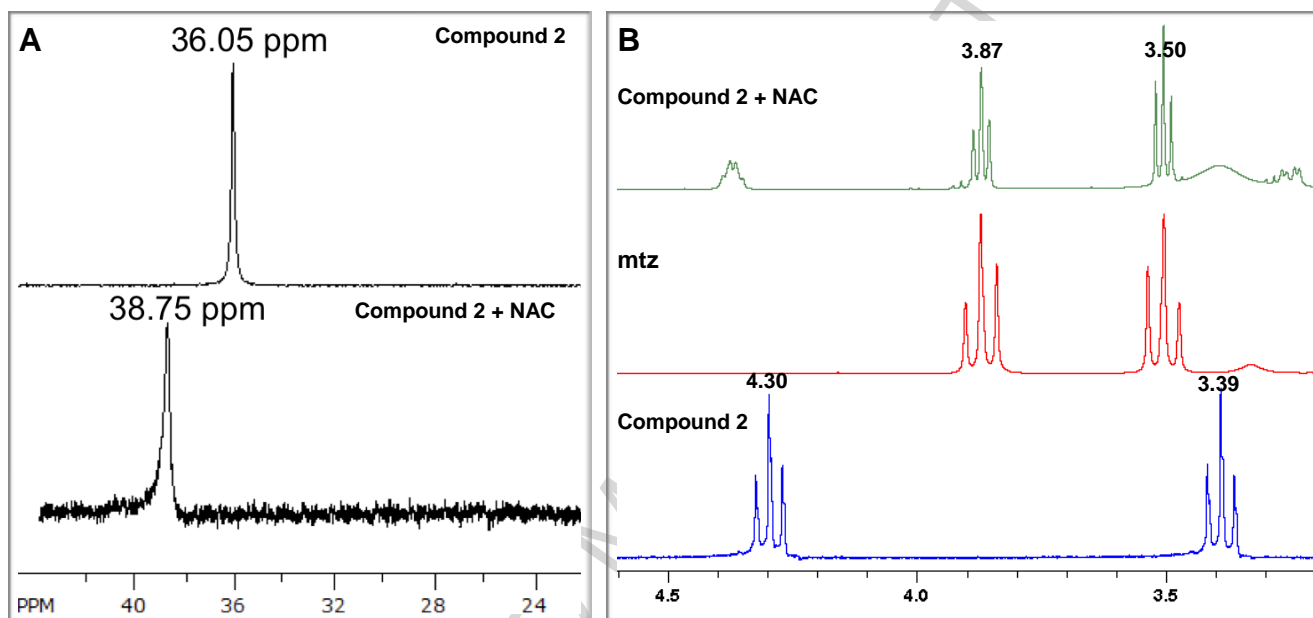


Figure 3

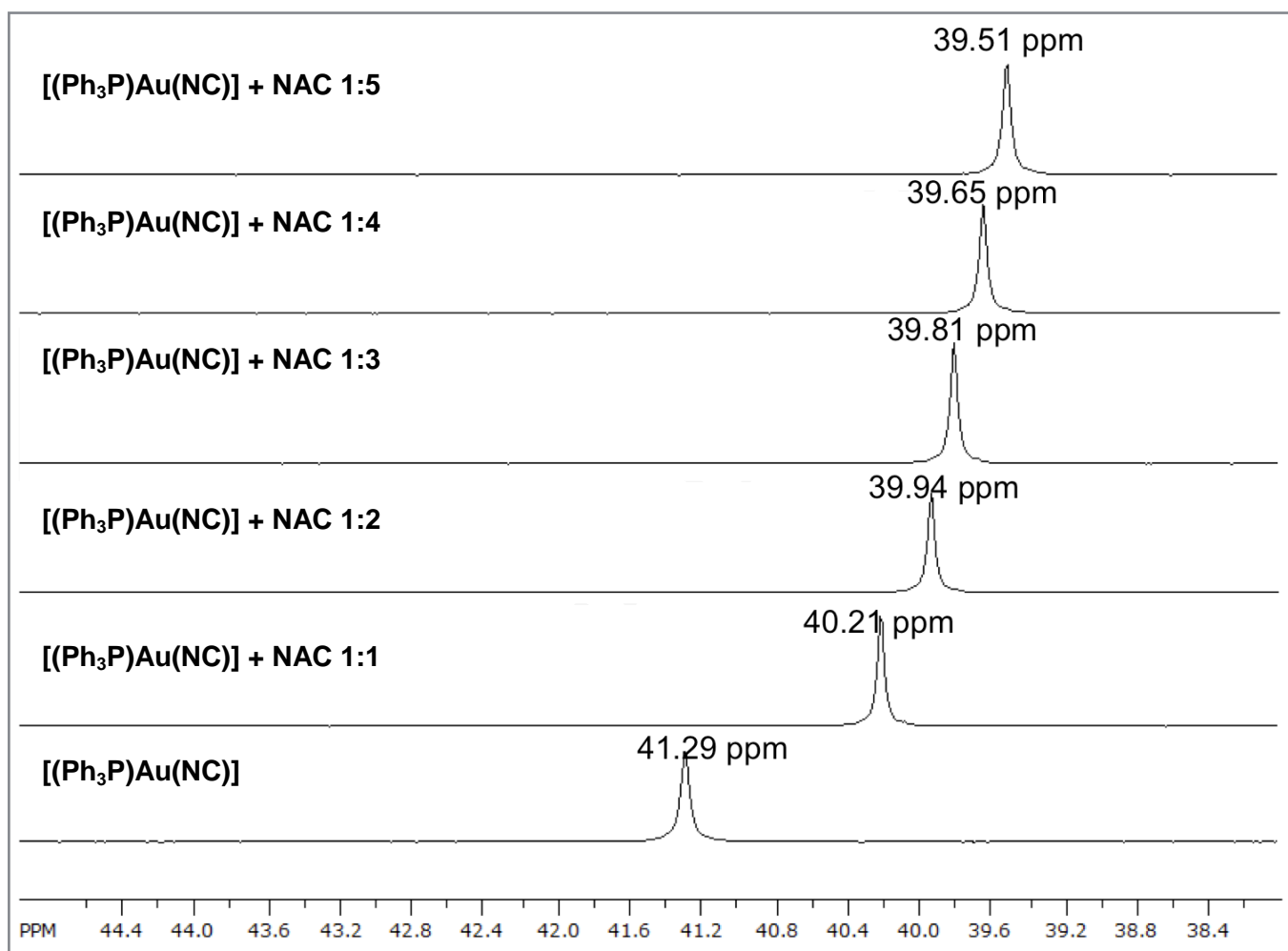


Figure 4

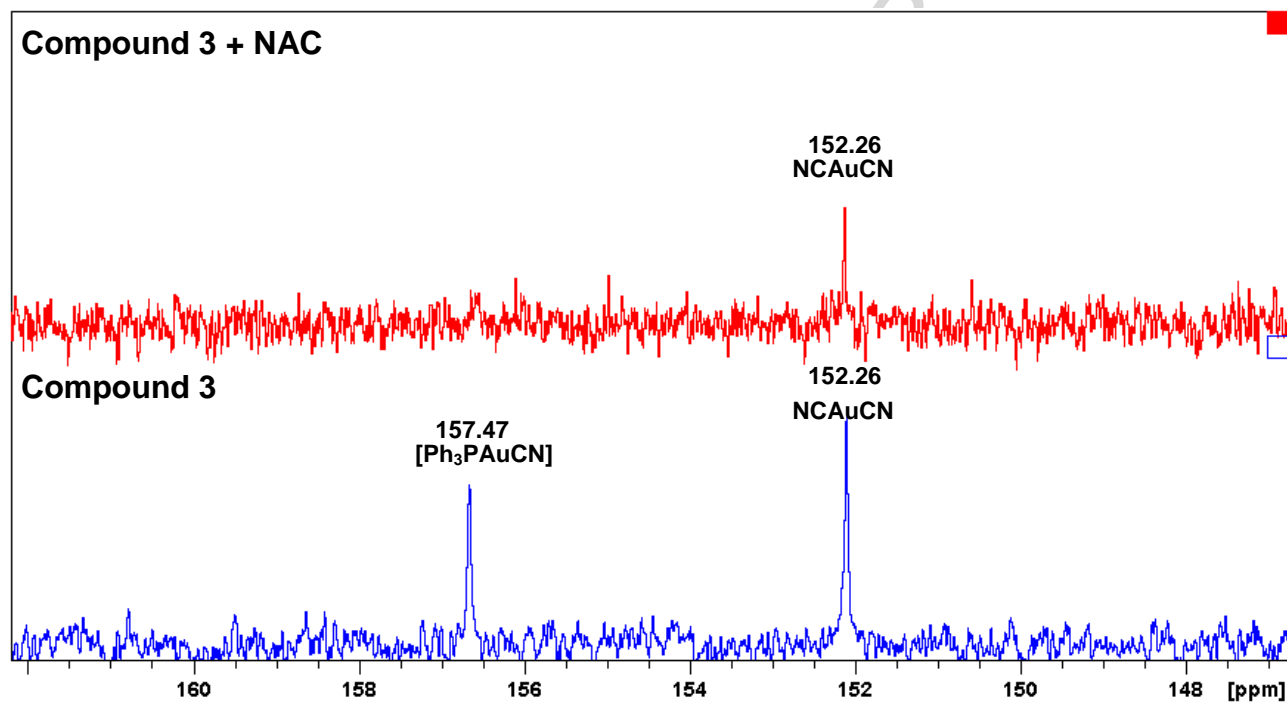


Figure 5

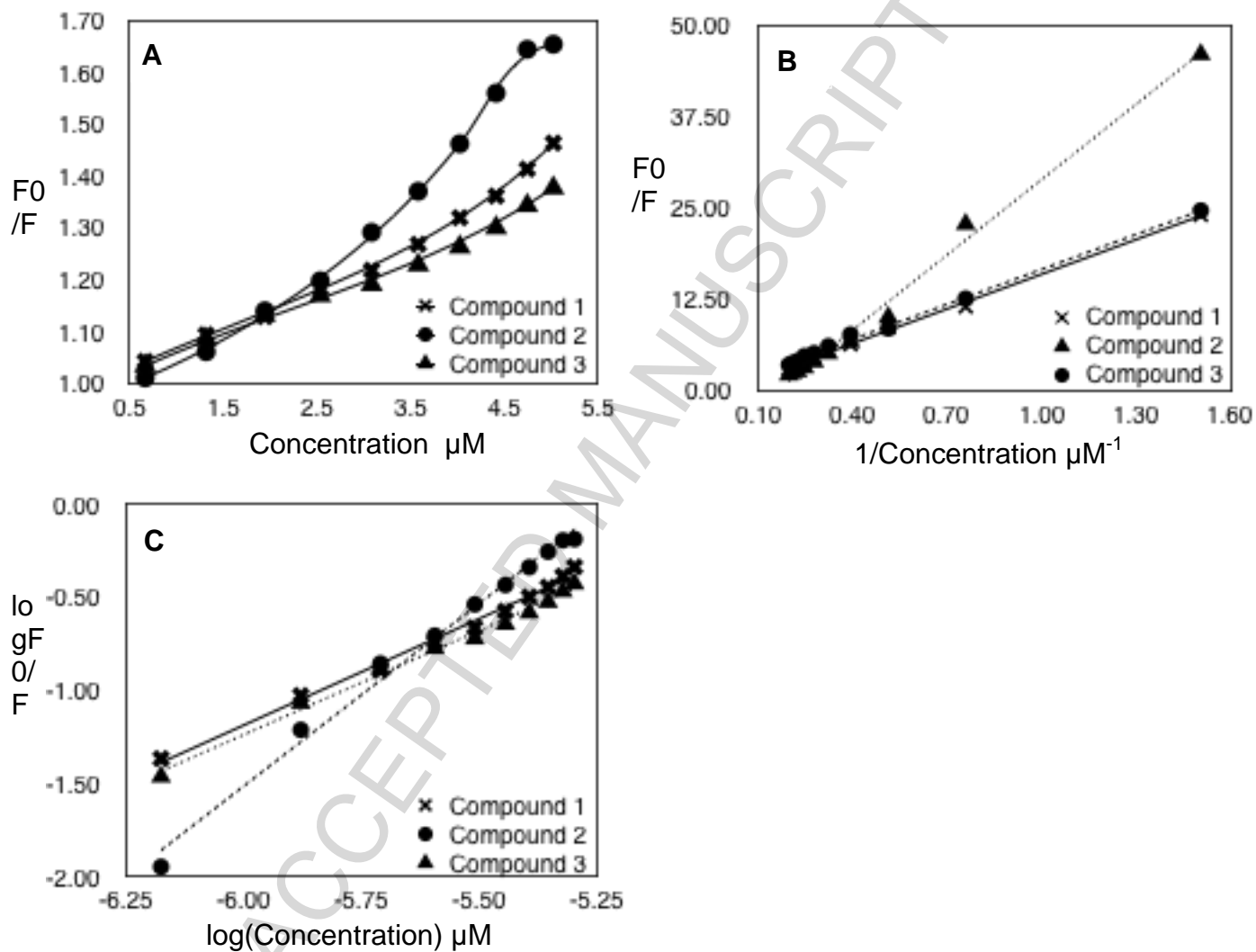
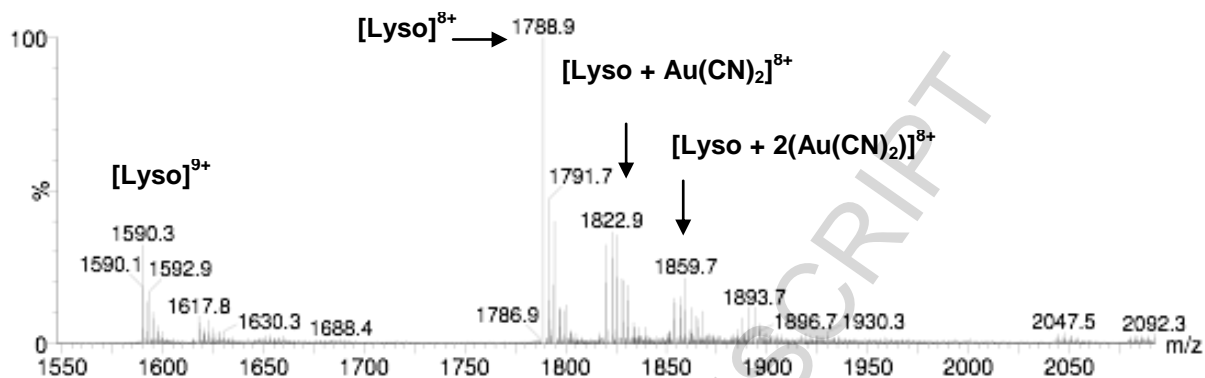
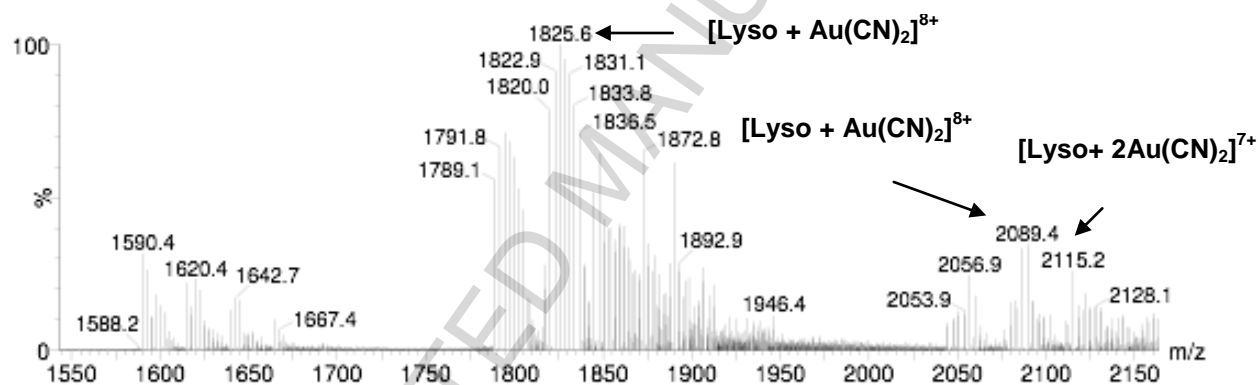


Figure 6

(C) Lysozyme + [(CN)Au(mtz)] - time 72h



(B) Lysozyme + [(CN)Au(mtz)] - immediate



(A) Lysozyme

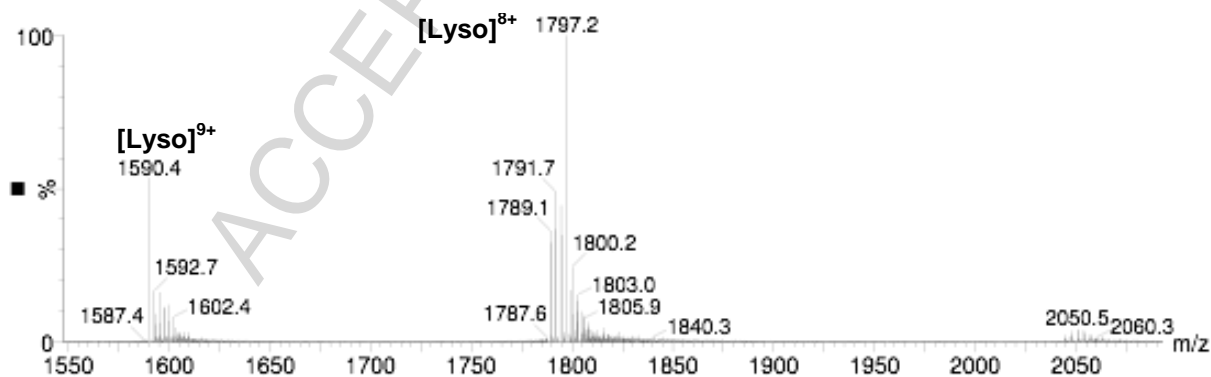


Figure 7

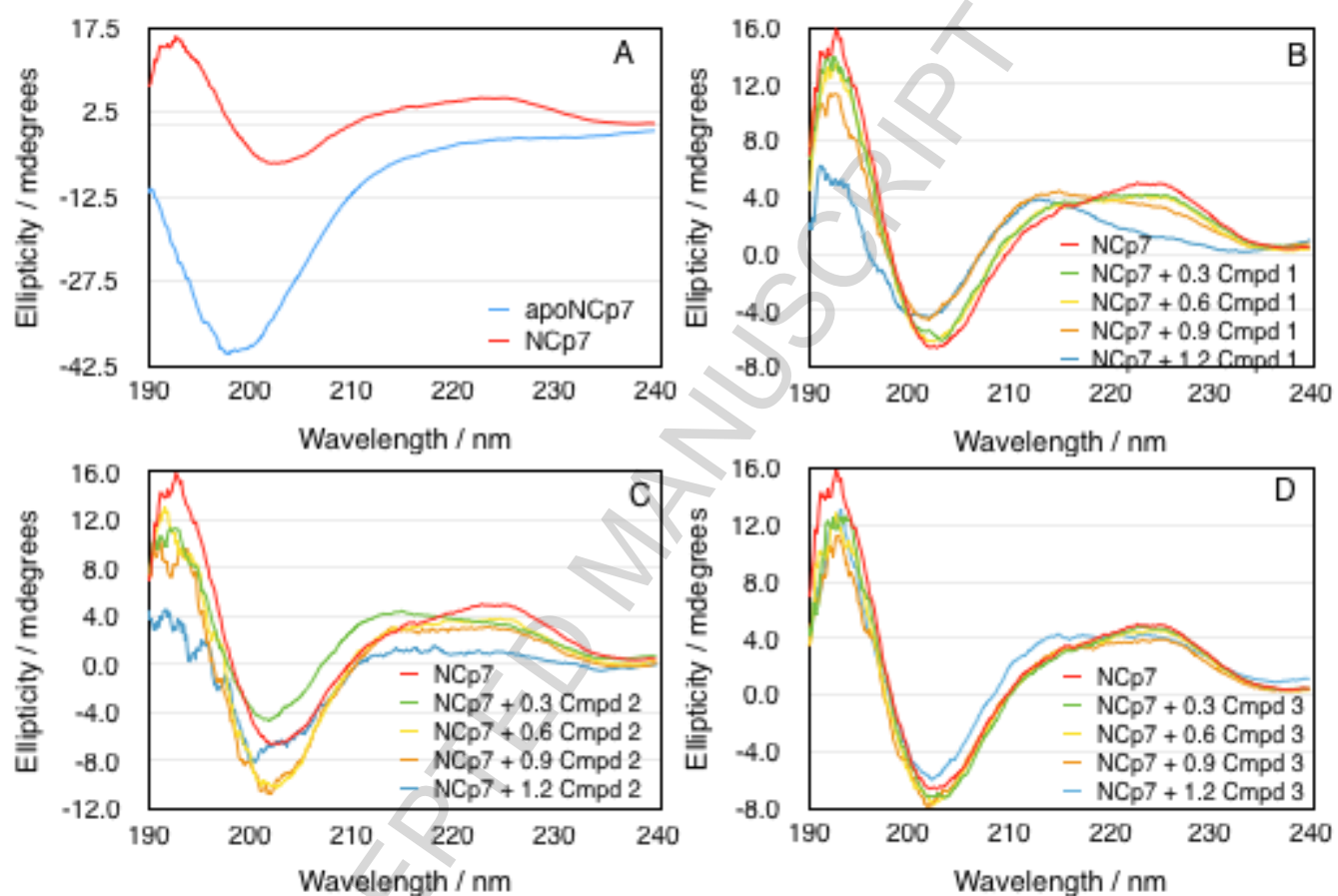
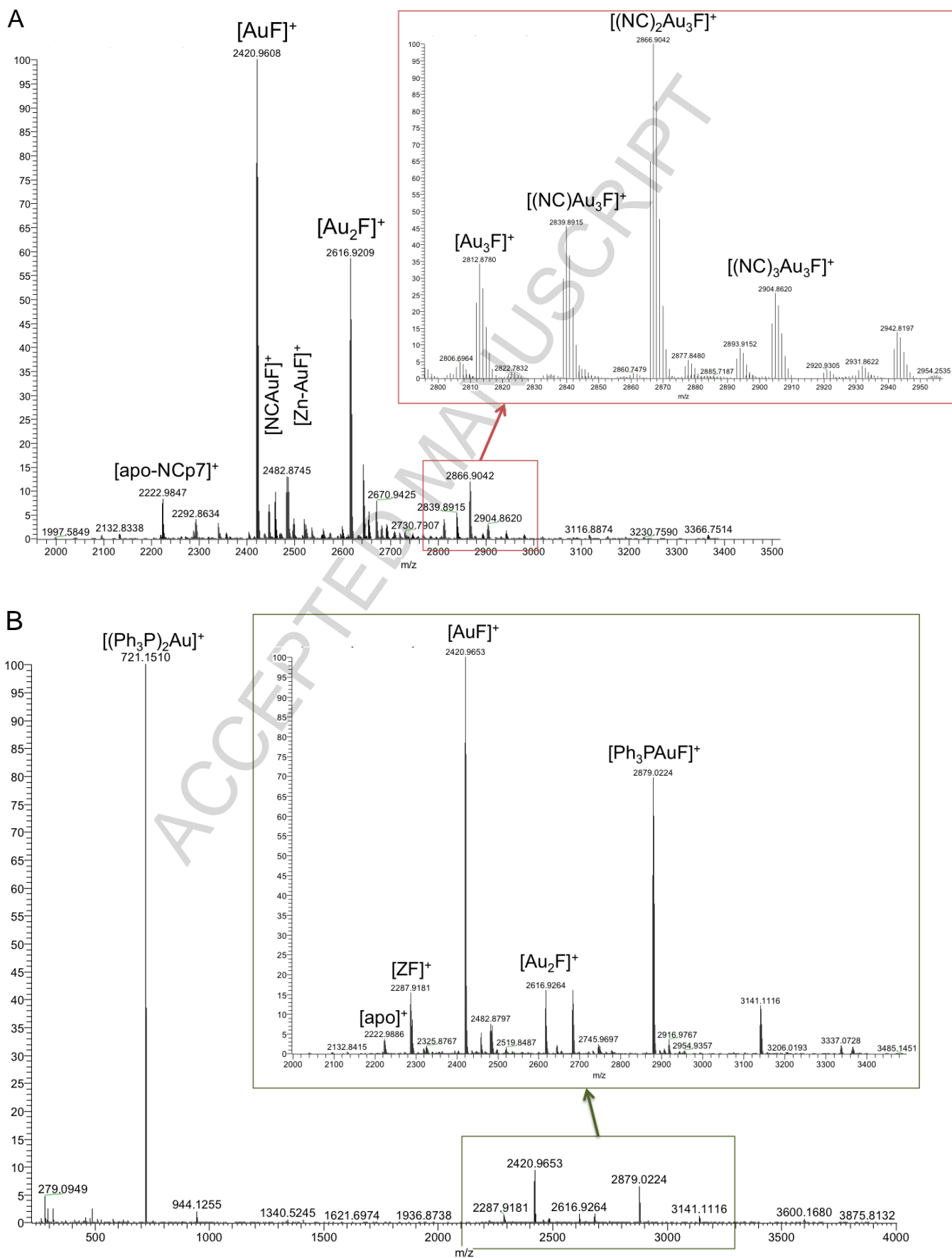


Figure 8



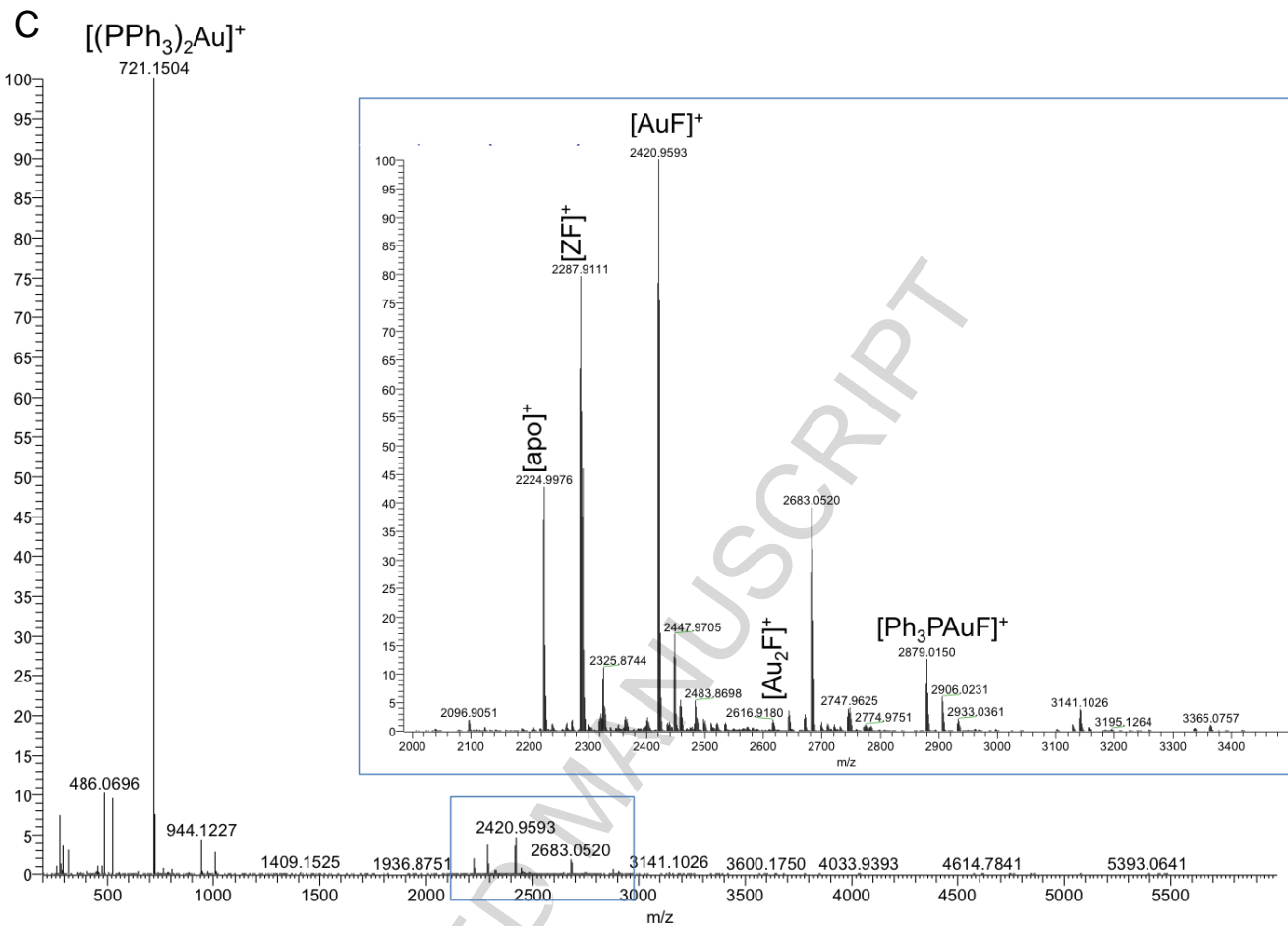


Table 1

Compound	$R^{2(a)}$	$K_a \times 10^4 (M^{-1})$	$R^{2(b)}$	n	$K_b \times 10^4 (M^{-1})$
1	0.998	6.330	0.992	1.140	6.708
2	0.993	2.919	0.992	1.960	2.305
3	0.997	6.293	0.993	1.110	4.702

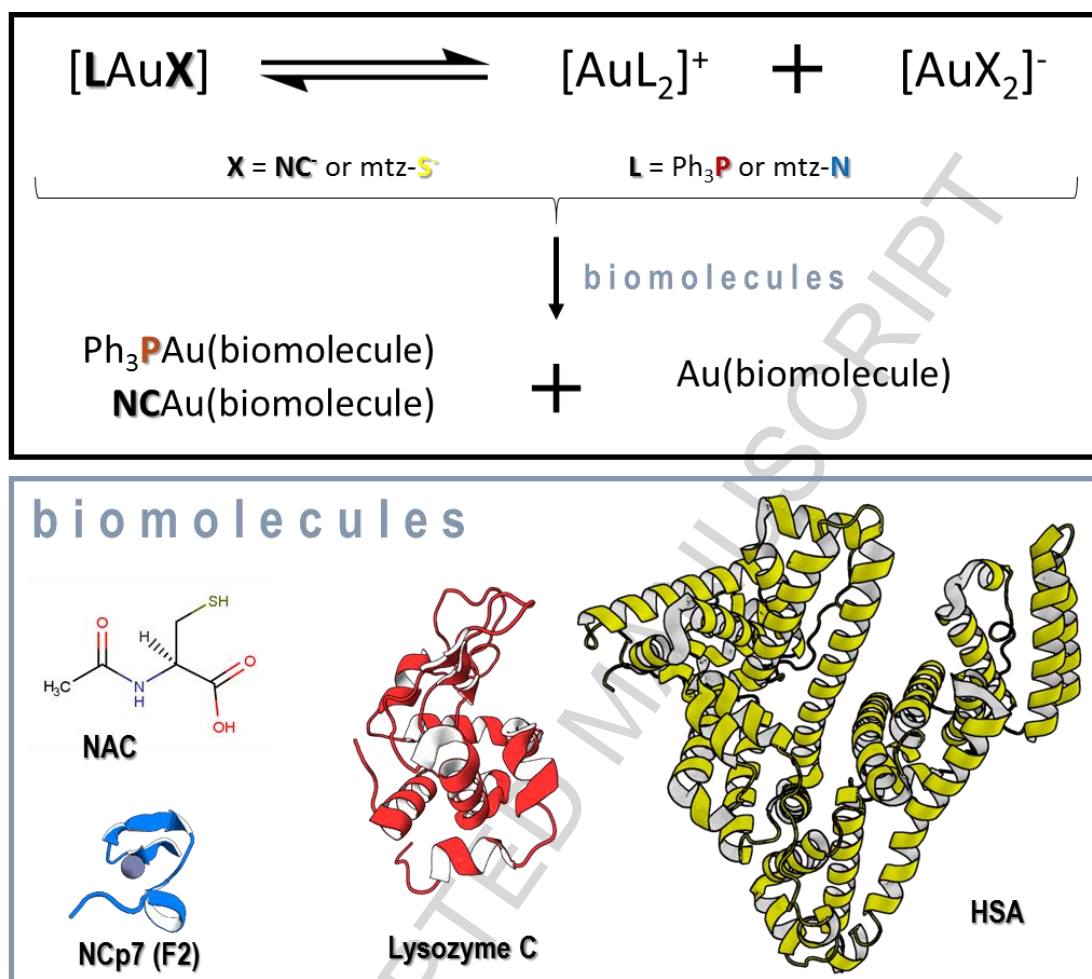
a:Coefficients of determination ( $R^2$ ) for the plot  $F/F_0$  versus  $1/\text{concentration}$  (Figure 5B) b:Coefficients of determination ( $R^2$ ) for the plot  $\log(F/F_0)$  versus  $\log \text{concentration}$  (Figure 5C).

Table 2

	IC <sub>50</sub> (μmol L <sup>-1</sup> )		
	Compound 1	Compound 2	Cisplatin
<b>HCT116</b>	2.7±0.2	2.2±0.2	7.6 ± 1.7
<b>MCF7</b>	1.0±0.1	1.9±0.4	4.8 ± 0.8
<b>A2780</b>	0.090±0.003	0.38±0.09	2.31 ± 0.06
<b>NG97</b>	11±1		
<b>HeLa</b>	< 2.00		15.14± 0.07 <sup>a</sup>
<b>3T3</b>	21.3±0.9		>100

<sup>a</sup> From ref. 48.

## Graphical abstract

Synopsis - Graphical Abstract – Abbehausen *et.al.*

Schematic representation of general ligand scrambling reaction of gold(I) linear compounds and interaction with sulfur containing biomolecules.

## Research Highlights

► In cyanogold complexes the  $\{(NC)Au(I)\}$  unit is coordinated to the zinc finger peptide. ► Lysozyme showed most differential reactivity toward Au(I) compounds. ► Interaction of gold(I) 2-mercaptothiazoline compounds with sulfur proteins can be modulated by the ligands and coordination mode. ► Different reactivity was found for gold(I)-2-mercaptothiazoline-phosphine and gold(I)-2-mercaptothiazoline-cyanide ► The gold(I)-2-mercaptothiazoline-cyanide compound demonstrated selective cytotoxicity.

ACCEPTED MANUSCRIPT